Hindawi Publishing Corporation
Mathematical Problems in Engineering
Volume 2015, Article ID 501401, 10 pages
http://dx.doi.org/10.1155/2015/501401

Research Article

Numerical Study on Infrared Optical Property of Diffuse Coal Particles in Mine Fully Mechanized Working Combined with CFD Method

Wen-Zheng Wang,[1] Yan-Ming Wang,[1,2] Guo-Qing Shi,[1] and De-Ming Wang[1]

[1]*School of Safety Engineering, China University of Mining and Technology, Xuzhou 221116, China*
[2]*Department of Mechanical and Aerospace Engineering, Rutgers, The State University of New Jersey, Piscataway, NJ 08854, USA*

Correspondence should be addressed to Yan-Ming Wang; cumtwangym@163.com

Received 14 July 2014; Revised 7 October 2014; Accepted 10 October 2014

Academic Editor: Hong-Liang Yi

Coal dust seriously threatens the safety and occupational health of coal mines. Numerical simulation research on the infrared radiation characteristics of diffused coal dust is carried out in fully mechanized working faces based on the optical monitoring problem of dust particles in mine atmospheric environments. The CFD method is applied to obtain the law of dust transport and distribution. Combined with Mie scattering model, the infrared radiation change characteristics and spectral selection of diffused coal dust particles are simulated and analyzed along the working face. The comparison results show the following: the attenuation and scattering characteristics of mine dust particles system are first enhanced, and then they weaken as the distance from dust source increases. The infrared attenuation of mine dust at the center of the vertical cross-section is generally greater than that at the roof and floor in the same location. The dispersion of mine dust directly determines the attenuation contribution of respirable dust to total dust. Moreover, the infrared absorption effect of functional groups in coal causes the infrared attenuation effect of coal dust to have obvious optical selectivity along the roadway, the existing optical "window."

1. Introduction

Coal mine dust is the solid phase particle generated during the mining operations of crushing, tunneling, extraction, and coal transportation [1]. The generated dust particles diffuse gradually with the mine ventilation system, polluting the entire mine atmospheric environment. Relevant studies in existing literature have shown that dust, especially respirable dust, is the main cause of coal worker's pneumoconiosis; some factors that increase the risk of developing pneumoconiosis are respirable dust concentration, particle size, exposure duration, and the chemical composition of dust particles [2–5]. In addition, coal dust particles are explosive in certain conditions such as appropriate temperature and oxygen may lead to coal-dust explosion or gas and coal-dust explosion accident [6–8]. According to relevant statistics, without dust prevention measures, dust concentration in fully mechanized caving faces reached 2,500–3,000 mg/m^3; the dust concentration in fully mechanized driving faces also reached 500 mg/m^3 [9], which significantly exceeds relevant state health standards [10]. Therefore, the theory and experimental research on dust pollution in mine atmospheric environments have important practical significance.

Domestic and foreign scholars have done much research on dust particles distribution and migration. The main research methods involved include sampling analysis at the scene and computer numerical simulation. Relevant research shows that, at the scene, dust generated in the working face diffuses gradually with the airflow in the tunnel, which presents a nonlinear change tendency [11]. At the same time, through the interaction of gravity and buoyancy lift, dust with different particle sizes experiences trajectory separation during the flow process in the mine atmosphere [12]. CFD simulation studies based on coal mining conditions confirmed the change phenomenon; moreover, the diffusion and deposition of dust have a larger relationship with the mine ventilation system [11, 13].

Given that dust particles in coal mine roadways seriously threaten the safety and occupational health of coal mine, the theory and method of mine dust prevention have become a popular research topic at present. In addition, the monitoring and evaluation of dust particle concentration is the precondition of mine dust prevention and control. The traditional dust filter membrane method does not meet the requirements for underground online analysis. Some researchers are already attempting to apply optical methods for detecting and monitoring mine dust [14, 15] and preliminarily formed the light scattering analysis method for dust concentration and granularity [16]. Given the particle distribution by existing industry analysis methods, they tied the light scattering properties of dust and particle projection section (or particle concentration) for a simple proportional relationship, which assumes that the light refraction parameter of particles is a constant value. The optical radiation of actual mine dust, especially coal particles and other minerals, is closely linked to its degree of carbonization and organic ingredients [17–19]. Thus, this simple hypothesis may cause big measurement errors. At the same time, existing mine dust optical measurement technology adopts the gas collecting sampling method. Interfering with the airflow outside, which distorts the concentration measurement, is inevitable. Moreover, the method can only sample several limited points but cannot monitor the nonlinear distribution change of mine dust in long wall faces and roadways in real time.

In summary, to effectively and accurately monitor and assess the pollution level of mine dust, the dust composition and its optical properties in roadways must first be thoroughly investigated, subsequently, the optical radiation characteristics simulation model [20–22] of mines must be set up based on the distribution regularity of dust in roadways, and, finally, mine dust comprehensive analysis system can be formed.

This paper adopts the CFD method to conduct a simulation research on mine dust particle pollution in typical fully mechanized working faces based on mine dust diffusion and distribution data in roadways, given the optical constants of mine dust particle according to the actual conditions of coal seam occurrence. The Mie scattering model is also used to set up the quantitative analysis method of mine dust optical radiation characteristics. This study is conducted to investigate the variations in attenuation, scattering, and transmission characteristics of dispersed particle systems as spectrum and distance change along the roadway in typical fully mechanized working faces.

2. Model and Formula

2.1. Mine Dust Particles Migration Model. To study the distribution and migration regularity of dust particles in the mine atmosphere, considering the release conditions of mechanical work dust source in fully mechanized working faces, this section establishes the mine atmosphere-dust coupled flow mathematical description along the tunnel based on gas-solid two-phase flow theory. Considering the characteristics of two-phase flows in the mine atmosphere, this paper establishes a flow control equation based on the Eulerian-Lagrangian model, which considers mine ventilation gas as a continuous phase and mine dust particles as a discrete phase.

Based on the assumptions above, we use the three-dimensional steady incompressible Navier-Stokes equation to describe the gas flow along the tunnel in fully mechanized working faces [23]. We also use the k-ε model to describe the turbulence effect and ignore heat transfer. Consequently, we obtain the following equations.

Continuous equation:

$$\frac{\partial}{\partial x_i}\left(\rho u_i\right) = 0. \tag{1}$$

Kinematic equation:

$$\frac{\partial}{\partial x_i}\left(\rho u_i u_j\right) = -\frac{\partial p}{\partial x_i} + \frac{\partial}{\partial x_i}\left[\left(\mu + \mu_t\right)\left(\frac{\partial u_j}{\partial x_i} + \frac{\partial u_i}{\partial x_j}\right)\right]. \tag{2}$$

k equation:

$$\frac{\partial}{\partial x_i}\left(\rho u_i h\right) = \frac{\partial}{\partial x_i}\left[\left(\mu + \frac{\mu_t}{\sigma_k}\right)\frac{\partial h}{\partial x_i}\right] + P_k - \rho\varepsilon. \tag{3}$$

ε equation:

$$\frac{\partial}{\partial x_i}\left(\rho u_i \varepsilon\right) = \frac{\partial}{\partial x_i}\left[\left(\mu + \frac{\mu_t}{\sigma_\varepsilon}\right)\frac{\partial h}{\partial x_i}\right] + \frac{O_{\varepsilon 1}\varepsilon}{h}P_k - O_{\varepsilon 2}\rho\frac{\varepsilon^2}{h}. \tag{4}$$

Among them,

$$\begin{aligned} \mu_t &= O_\mu \rho \frac{h^2}{\varepsilon}, \\ P_k &= \mu_t \frac{\partial u_j}{\partial x_i}\left(\frac{\partial u_j}{\partial x_i} + \frac{\partial u_i}{\partial x_j}\right), \end{aligned} \tag{5}$$

where P_k is the turbulent kinetic energy change rate of shear force, h is the turbulent kinetic energy, $\mathrm{m}^2/\mathrm{s}^2$, ε is the turbulent kinetic energy dissipation rate, $\mathrm{m}^2/\mathrm{s}^3$, μ is the laminar viscous coefficient, Pa·s, μ_t is the turbulence viscosity coefficient, Pa · s, p is the turbulent effective pressure, Pa, ρ is the quality of volume of gas, $\mathrm{kg/m}^3$, x_i are the coordinates of the x, y, and z directions, m, u_i are the speed of the x, y, and z direction, m/s, and $O_{\varepsilon 1}$, $O_{\varepsilon 2}$, and O_μ are empirical constants whose values are 1.44, 1.92, and 0.09, respectively. σ_ε and σ_k are Prandtl number corresponding to the turbulent kinetic energy and turbulent kinetic energy dissipation rate whose values are 1.3 and 1.0, respectively.

Given that the gas phase flow model is established, we introduce a discrete phase model to describe the force balance effect of dust particles suspended in the mine atmosphere. The equation can be defined as

$$m_p \frac{du_p}{dt} = \Sigma F = F_d + F_g + F_f + F_s + F_b + F_x, \tag{6}$$

where m_p is the particle mass, kg, u_p is the particle velocity, m/s, ΣF is the particle total force, N, F_d is the particle motion

resistance, N, F_g is the particle gravity, N, F_f is the particle buoyancy, N, F_x is the other force, N, and added mass force, Magnus lift, thermophoresis force, Saffman lift, Brown, and so on are included. The order of magnitude of these forces is very small and ignored in the paper. Consider

$$F_d = \frac{1}{2} O_d O_p A_p \rho \left(u_g - u_p\right) \left|u_g - u_p\right|, \tag{7}$$

where O_d is the resistance coefficient, O_p is the dynamic shape coefficient, according to the dispersion experiment data, here taking 1, A_p is the windward area of particle, m^2, u_g is the airflow velocity, m/s, u_p is the particle velocity, m/s, and O_d is the resistance coefficient associated with the Reynolds number of particles. Consider

$$\begin{aligned} O_d &= f\left(\mathrm{Re}_p\right), \\ \mathrm{Re}_p &= \frac{\rho d_p \left|u_g - u_p\right|}{\mu}, \end{aligned} \tag{8}$$

where Re_p is the Reynolds number, dimensionless, and d_p the particle diameter, m.

We solve the particle tracks through the integral differential equation of particle forces in the Lagrangian coordinate. Sufficient representative particle trajectory is calculated to obtain the law of particle movement and diffusion as well as the distribution in continuous phase.

2.2. Optical Radiation Model of Mine Dust Particles. The two-phase flow model in coal mines have been discussed above. We can obtain the distribution and migration regularity of dust particles along the tunnel in fully mechanized working faces using calculations. The calculations are made according to the simulation results of particle concentration and dispersion in different locations along working faces. Combined with the theory of particle radiation, we can obtain the variation in the attenuation and scattering characteristics of dust along the tunnel.

This paper adopts Mie scattering model to calculate the attenuation factor, scattering factor, scattering albedo, and scattering phase function of single mine dust particles [24, 25]. Its formula is

$$\begin{aligned} Q_e(m,\chi) &= \frac{C_e}{G} = \frac{2}{\chi^2} \sum_{n=1}^{\infty} (2n+1)\,\mathrm{Re}\left(a_n + b_n\right) = \frac{4}{\chi^2}\,\mathrm{Re}\left\{S_0\right\}, \\ Q_e(m,\chi) &= \frac{C_s}{G} = \frac{2}{\chi^2} \sum_{n=1}^{\infty} (2n+1)\left[\left|a_n\right|^2 + \left|b_n\right|^2\right], \\ w_p &= \frac{Q_s}{Q_e}, \\ \Phi_p = (m,\chi,\theta) &= \frac{1}{Q_s \chi^2}\left[\left|S_1\right|^2 + \left|S_2\right|^2\right], \end{aligned} \tag{9}$$

where m is the particle optical constant, $m = n - ik$, n and k are refractive index (single refractive index) and absorption index, respectively, χ is the size parameter $\chi = \pi D/\lambda$, G is the geometric projection area of the spherical particles, $G = \pi D^2/4$, m^2 or μm^2, w_p is the scattering albedo of single particle, Φ_p is the scattering phase function of single particles, θ is the scattering angle, Re is taking the real component of plural, a_n and b_n are the Mie scattering coefficients, S_1 and S_2 are the complex amplitude functions, S_0, $S_1(0)$, and $S_2(0)$ are the prior amplitude functions, $S_0 = S_1(0) = S_1(0)$.

The particle swarms of mine dust in any location along the tunnel in working faces are composed of a series of different scale particles. The optical radiation parameters of nonuniform particle swarm can be given by the following formula:

$$\begin{aligned} \beta_\lambda &= \int_0^\infty C_{e\lambda}(D)\, N(D)\, dD, \\ \kappa_\lambda &= \int_0^\infty C_{\alpha\lambda}(D)\, N(D)\, dD, \\ \sigma_{s\lambda} &= \int_0^\infty C_{s\lambda}(D)\, N(D)\, dD, \end{aligned} \tag{10}$$

where D is the particle size, m or μm, $C_{e\lambda}(D)$, $C_{\alpha\lambda}(D)$, and $C_{s\lambda}(D)$ are the attenuation, absorption, and scattering cross-section of a particle with the diameter of D, $N(D)$ is the particle number density distribution, $m^{-3} \cdot m^{-1}$ or $m^{-3} \cdot \mu m$.

Due to the common industrial analysis of coal dust, the nonuniform size dust particles are generally divided into several size ranges for statistics. Therefore, the discrete integration is employed to approximate the continuous number density function in this paper and the middle diameters of each particle group are selected as equivalent diameters for calculation to approximate the above equations.

3. Mine Dust Distributions along the Fully Mechanized Working

3.1. Geometry Model and Parameters Configuration. This paper adopts CFD method to create a numerical simulation on a typical fully mechanized working face in the Wuda mining area, northwest China. Because there are coal-cutting machine, supporting equipment, and cable tray on the fully mechanized working face, the model becomes so complicated that setting up an exact geometric model becomes impossible. Thus, the calculation area is simplified and a cuboid calculate area of 100 m * 4 m * 3 m is set up. A 5 m * 2 m * 1.2 m coal-cutting machine is set up and simplifies the supporting equipment as four cylinders. Then, grid plotting is accomplished as shown in Figure 1.

According to the characteristics of two-phase flow in fully mechanized working face combined with the mathematic model, we set up the main index of data simulation and boundary condition as follows. Solver: segregated, viscous model: k-epsilon, discrete phase model: on, material: coal-ml, and diameter distribution: Rosin-Rammler, min. Diameter: 1×10^{-7} m, max. diameter: 5×10^{-5} m, mean diameter: 7×10^{-6} m, spread parameter: 1.05, total flow rate: 0.008 kg/s, inlet boundary type: velocity inlet, inlet velocity magnitude:

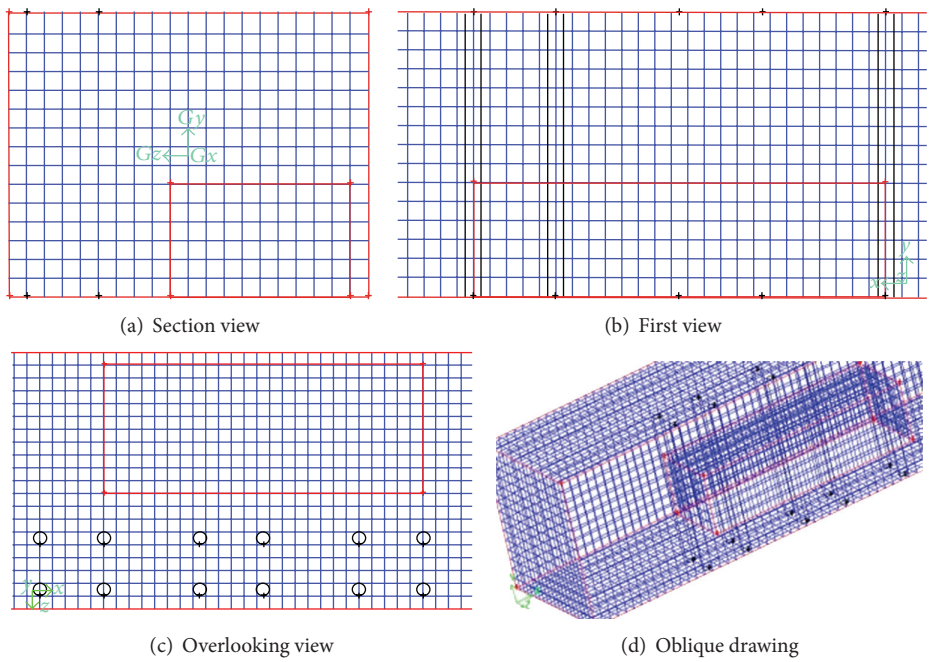

(a) Section view (b) First view

(c) Overlooking view (d) Oblique drawing

Figure 1: Geometry model and grid plotting grid of fully mechanized working face.

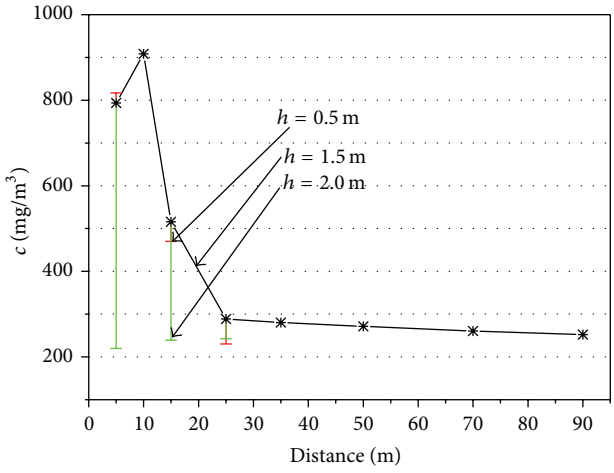

Figure 2: Simulation of dust concentration variation in two-dimensional direction.

2 m/s, and outlet boundary type: outflow. Then, the computation based on the conditions above is simulated.

3.2. Simulation Results. According to the established model combined with CFD method, we carried out the numerical simulation on mine dust particle diffusion phenomenon along the tunnel in fully mechanized working face with the mechanical work dust source. The mine dust concentration and dispersion distribution in the direction of along the tunnel (5 m to 90 m from dust source) and the vertical direction (0.5 m, 1.5 m, and 2.0 m above the floor) are obtained, respectively. The numerical results are shown in Figure 2 as well as Tables 1 and 2.

Table 1: Simulation results of dust particle dispersion in the direction along the tunnel.

Distance (m)	Dust dispersion degree (%)			
	<2 μm	≥2~5 μm	>5~10 μm	>10 μm
5	23.5	23	36.5	17
10	26	25	33.4	15.6
15	30	29	30.5	10.5
25	39.5	33.5	22.5	4.5
35	41	39.5	11	8.5
50	44.5	40	12.5	3
70	69.5	25.5	3.5	1.5
90	75	15	7.5	2.5

Figure 2 shows the presence of a slight increase in the dust concentration, which is 1.5 m above the floor, from 5 m to 10 m. Then, dust concentration declined sharply. After 25 m, dust concentration remains almost stable. Particles settle gradually under the force of gravity during the process of diffusion, which leads to the variation of dust concentration in the vertical direction. Along with the increase of distance from dust source, large particles gradually settle completely. Small particles diffuse with airflow. The variation of dust concentration in vertical direction becomes smaller and smaller and gradually becomes stable.

Under the background of coal dust analysis, the nonuniform particle sizes are separated into four ranges: <2 μm, ≥2~5 μm, >5~10 μm, and >10 μm. The simulation results of dust particle dispersion in two-dimensional direction are shown in Tables 1 and 2.

Table 2: Simulation results of dust particle dispersion in vertical direction.

Distance (m)	Vertical height (m)	Dust dispersion degree (%)			
		<2 μm	≥2~5 μm	>5~10 μm	>10 μm
5	0.5	16	22	42	20
	1.5	22.5	23	37.5	17
	2	28	33.5	33	5.5
15	0.5	30	30.5	27.5	12
	1.5	30	29	31.5	9.5
	2	32	29	35	4
25	0.5	33.5	28.5	31.5	6.5
	1.5	39.5	32.5	23.5	4.5
	2	38	27.5	31	3.5

Table 3: Industrial analysis of some coal seams in Wuda mining area.

Coal seam	M (%)	A (%)	V (%)	Fc (%)
15#	1	26.05	27.18	45.77
16#	0.76	36.7	30.36	32.18
17#	0.74	33.9	29.87	35.49

4. Optical Constants of Coal Dust Particles

The typical fully mechanized working face in Section 2 is located in the Wuda mining area, Northwest China. Its coal era is the Carboniferous Taiyuan group, Upper Palaeozoic group, and Permian Shanxi group, which contain 27 coal seams in total. The fully mechanized working face is located in the 16# coal seam. The industrial analysis of some coal seams is shown in Table 3.

Analyzing the coal seam above, we can find that the mine dust particles in fully mechanized working face should be bituminous coal particles according to the degree of coal metamorphism.

Currently, many related reports on the optical radiation of pulverized coal particle are available. Previous studies [17, 18, 26] conducted a systematic study on the optical radiation characteristics of coal, ash, and carbon black particles using a coal-fired boiler and a combustion chamber based on Mie scattering theory. According to the infrared transmission experiment data of coal particles, we can obtain the complex refractive index of coal particles in different wavelengths through the inversion method. In this paper, according to the data provided in [26], we obtain the optical constants of bituminous coal particles and list the complex refractive index data under the spectral range of 2–25 μm in Table 4.

This paper assumes the dust particles to be homogeneous spherical particles whose physical properties are the same in all directions. On the basis of determining the complex refractive index of coal particle combined with the Mie scattering model mentioned above, the attenuation, scattering factor spectrum distribution characteristics of mine dust are calculated as shown in Figures 3 and 4.

Figure 3 shows the following: within the wavebands 2–25 μm, the attenuation characteristic of medium size dust particles (2 μm–10 μm) is far stronger than small particles (0 μm–2 μm). The attenuation characteristic of the mine dust whose particle size is less than 10 μm peaks at the spectral ranges of 2–5, 8–12, and 20–25 μm respectively. In addition, the spectral peak moved towards the long wave as particle size increased. The minimum point of attenuation factor occurs at around 8 μm. Large particles with sizes of more

Table 4: Complex refractive index of bituminous coal particle under different wavelengths.

Wavelength (μm)	n	k
2	1.51971	0.00092
3	1.50702	0.02015
4	1.4925	0.00366
5	1.45736	0.00521
6	1.39768	0.01306
7	1.32044	0.0075
8	1.071	0.06951
9	1.14862	0.80971
10	1.85831	0.65411
11	1.72159	0.21717
12	1.57001	0.18863
13	1.64885	0.23381
14	1.59346	0.18055
15	1.5354	0.21549
16	1.50283	0.30231
17	1.48859	0.38969
18	1.46852	0.4186
19	1.45142	0.44569
20	1.3968	0.52381
21	1.42626	0.68305
22	1.57382	0.93501
23	1.7657	0.95984
24	1.81469	0.91042
25	1.57361	0.78529

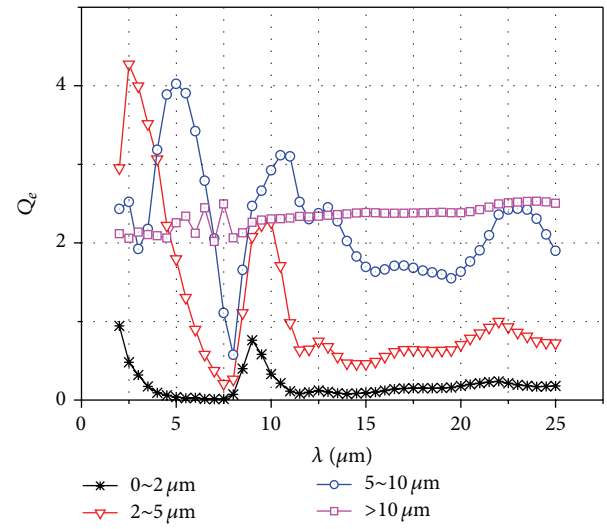

Figure 3: Attenuation factor of bituminous coal.

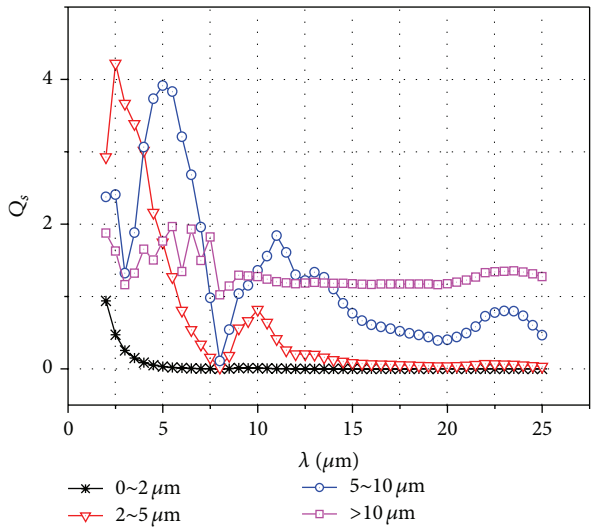

Figure 4: Scattering factor of bituminous coal.

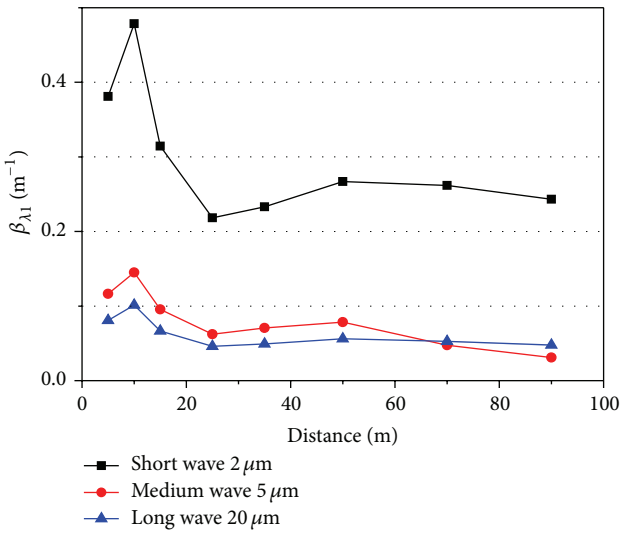

Figure 5: Attenuation coefficient variation of respirable dust along the tunnel.

than 10 μm have scale factors greater than 1 under the spectral band. The particle is embodied in big particle scattering characteristics. Thus, its attenuation characteristics vary little with wavelength. A comparison of Figures 3 and 4 shows that the variation law of mine dust scattering is similar to its attenuation characteristic. Its scattering factor is significantly less than the attenuation factor when the wavelength is greater than 8 μm. This result suggests that the particulate absorption effect is significant within the spectral range.

5. Results and Discussion

The law of dust transportation and distribution with the optical radiation parameters of coal dust particles are combined. This paper adopts the Mie model to carry out numerical simulations for the optical radiation properties of dust particles in two-dimensional directions (along the tunnel and the vertical direction) of a working face roadway. Current studies on mine dust mainly concentrate on respirable dust and total dust. Thus, this section mainly analyzes these two kinds of dust particles.

5.1. Optical Radiation Properties Variation Law of Dust along the Working Face. According to the dust particles concentration and dispersion along the tunnel, combined with Mie scattering theory, we calculated and analyzed the optical radiation characteristics of respirable dust and total dust, respectively.

Figures 5 and 6 show a slight increase in the attenuation coefficient of respirable dust as the distance from the dust source increases. Then, it declines sharply until 25 m. Subsequently, it remains almost stable. This phenomenon anastomoses with the law of dust concentration distribution. In addition, the attenuation characteristics of mine dust under the shortwave spectrum are stronger than in other spectrums because the scale factor of respirable dust is greater than 1 under shortwave. Moreover, its forward scattering was

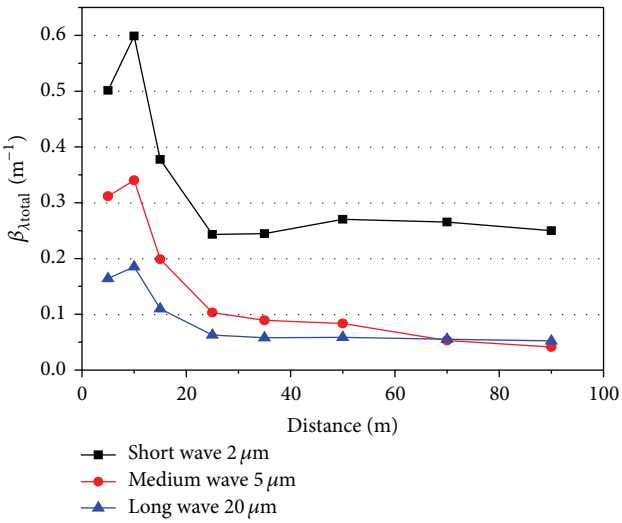

Figure 6: Attenuation coefficient variation of total dust along the tunnel.

greatly enhanced. The variation law of total dust attenuation characteristics along the tunnel is similar to respirable dust. The attenuation coefficient of total dust is larger than respirable dust under arbitrary wavelength. The optical radiation characteristics of total dust relatively increase due to the added radiation of large particles.

Figures 7 and 8 show that the variation law of dust particle scattering coefficient along the tunnel is similar to its attenuation coefficient. The scattering coefficient of dust particles obviously declines as the detection wavelength increases. The scale factor of mine dust is relatively small under the long wave. Its forward scattering effect has been seriously weakened. Thus, the scattering coefficients of dust particles gradually converge to 0.

When calculating the transmittance in this model, we choose to set detection light in the vertical direction of

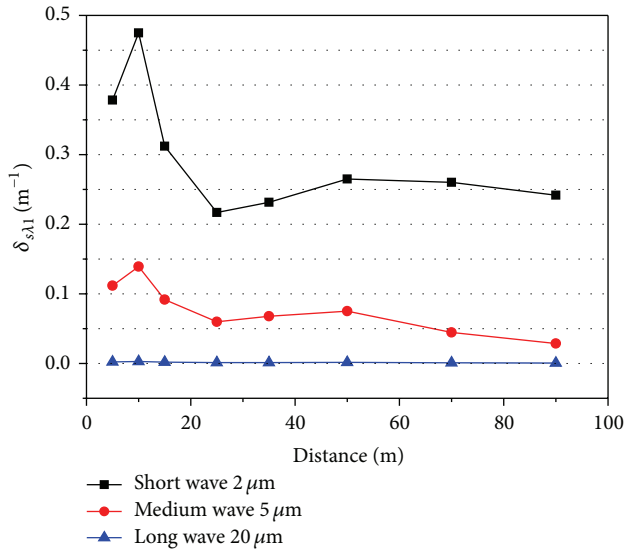

Figure 7: Scattering coefficient variation of respirable dust along the tunnel.

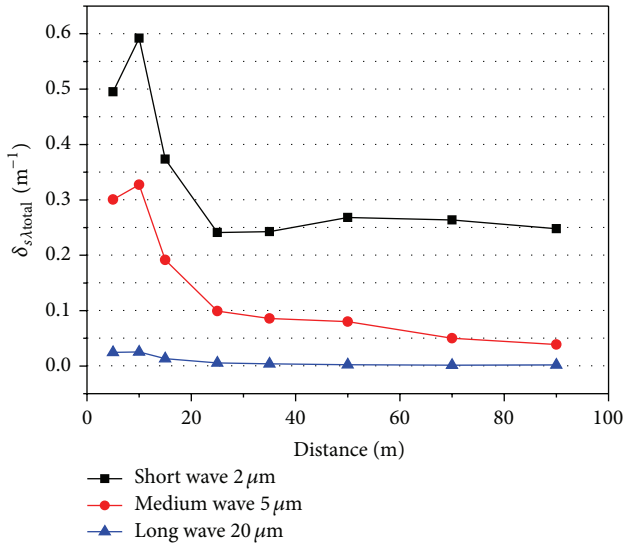

Figure 8: Scattering coefficient variation of total dust along the tunnel.

the coal wall and then summarize the data at each sampling point. As shown in Figure 9, X, Y, and Z are the direction of along the tunnel, the vertical direction from rook floor to roof, and the vertical direction of the coal wall, respectively. The red line is the detection optical path.

According to the simulation results of particle concentration and dispersion, we consider the particles distribution to be uniform in the vertical direction of the coal wall. When calculating the transmittance of particle in Z direction, the optical path is set to a constant value of 4 m. Based on the assumption above, according to the relationship formula between transmittance and the attenuation coefficient $\gamma_\lambda = \exp^{(-\beta_\lambda L)}$, we calculated and analyzed the variation law of

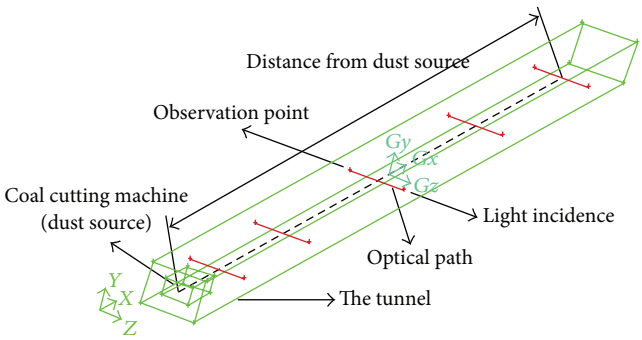

Figure 9: Detection point set of fully mechanized working face.

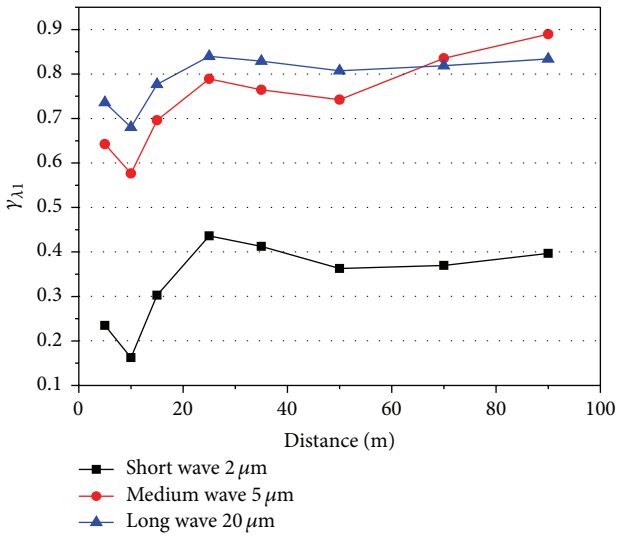

Figure 10: Transmittance variation of respirable dust.

particle transmittance along the tunnel, as shown in Figures 10 and 11.

Figures 10 and 11 show that the variation law of mine dust transmittance along the tunnel is negatively related to mine dust concentration distribution. When the dust is close to the dust source, the transmittance of mine dust under the shortwave spectrum is relatively small. This type of mine dust has a stronger attenuation effect for transmission signal. The transmittance of total dust is weaker than respirable dust along the tunnel due to the attenuation contribution of large particles. The transmittance of mine dust is in a nonlinear increase as the distance from dust source increases.

5.2. Optical Radiation Properties Variation Law of Dust in Vertical Direction. According to the simulation data of dust concentration and dispersion in the vertical direction, three sites (5, 15, and 25 m from dust source) are used as sampling sites, respectively. Mie scattering theory is also used to calculate and analyze the optical radiation characteristics of mine dust, which is 0.5, 1.5, and 2.0 m above the floor in the three sites, as shown in Table 5.

Table 5 shows that the attenuation characteristics of repairable dust at the center of the vertical cross-section

Table 5: The attenuation coefficient variation of dust in vertical direction.

Distance (m)	Height (m)	Attenuation coefficient (m^{-1})					
		Short wave (2 μm)		Medium wave (5 μm)		Long wave (20 μm)	
		Respirable dust	Total dust	Respirable dust	Total dust	Respirable dust	Total dust
5	0.5	0.3007	0.443177	0.107077	0.338284	0.06505	0.164312
	1.5	0.388	0.510316	0.118485	0.317494	0.08223	0.167009
	2	0.134	0.164073	0.046133	0.095648	0.02885	0.049264
15	0.5	0.2982	0.349042	0.091317	0.174017	0.06323	0.098513
	1.5	0.3442	0.413359	0.104511	0.217504	0.07289	0.120512
	2	0.1508	0.182536	0.044426	0.096703	0.03181	0.053326
25	0.5	0.14815	0.176031	0.04233	0.08807	0.03114	0.050194
	1.5	0.21324	0.237569	0.060843	0.100763	0.04482	0.061438
	2	0.16547	0.193223	0.043609	0.089247	0.03446	0.053331

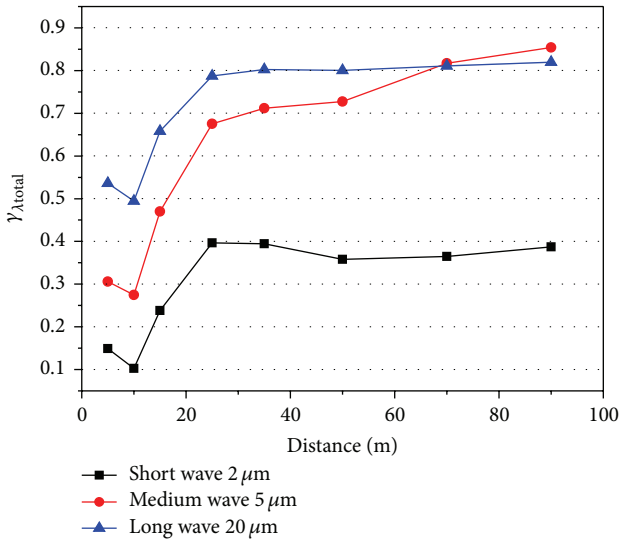

Figure 11: Transmittance variation of total dust.

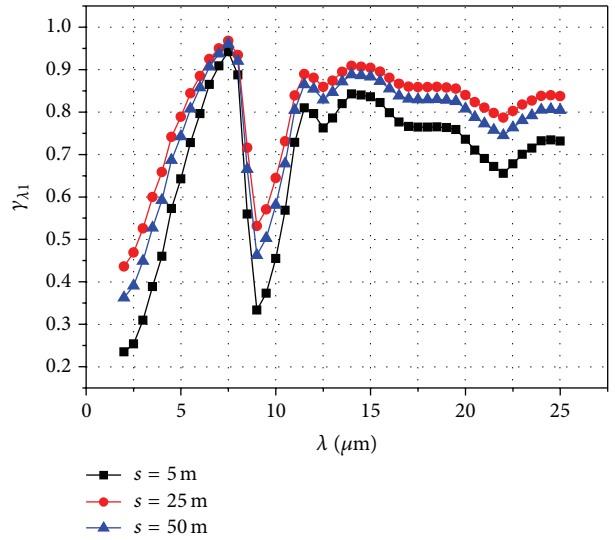

Figure 12: Transmittance variation of respirable dust under different wavelengths.

of roadway (1.5 m above the floor) are stronger than those near the roof and floor. The relationship of the attenuation coefficient between the particles at the roof and the particles at the floor is related to sampling sites and wavelength, which anastomoses with the law of dust concentration distribution in the vertical direction. The scale factor of mine dust is greater than 1 under shortwave. The enhanced forward scattering resulted in the particle with larger attenuation characteristics under shortwave.

The attenuation coefficient of total dust particles presents a similar variation law. Moreover, the total dust particles compound the radiation from large particles. Such radiation causes the attenuation coefficient of total particles to be larger than respirable dust.

The variation law of particle transmittance in vertical direction is calculated and analyzed in the same way, as shown in Table 6.

Table 6 shows that the variation law of dust transmittance is negatively related to mine dust concentration distribution and attenuation coefficient. The dust particle concentration is larger in the center of cross-section, which leads to the poor transmittance of particles and seriously influences the optical detection of mine dust particles.

5.3. The Relationship between the Spectral Selectivity and Distribution of Mine Dust. The study above analyzed the infrared radiation characteristics variation of dust particles, which disperse in the tunnel in the two-dimensional direction. The optical radiation characteristic of mine dust has obvious selectivity for wavelength and is directly linked to mine dust concentration and particle size distribution. Thus, this section selects three sites (5, 25, and 50 m from dust source, resp.) as sampling points. We calculate and analyze the transmittance of total dust and respirable dust under the band spectrum of 2–25 μm (data is taken from the cross-section center line).

Figures 12 and 13 show that the spectral transmittance of respirable dust and total dust has similar variation laws. The dust particle concentration is relatively high near the dust source (s = 5 m). As a result, the spectral transmittance is minimum. Meanwhile, the contribution to the attenuation of

Table 6: Transmittance variation of dust in vertical direction.

Distance (m)	Height (m)	Transmittance					
		Short wave (2 μm)		Medium wave (5 μm)		Long wave (20 μm)	
		Respirable dust	Total dust	Respirable dust	Total dust	Respirable dust	Total dust
5	0.5	0.3189	0.1856	0.6658	0.2766	0.7809	0.5355
	1.5	0.2289	0.1438	0.6374	0.2993	0.7317	0.5302
	2	0.601	0.5361	0.8392	0.6952	0.8961	0.8293
15	0.5	0.3219	0.2653	0.7068	0.5162	0.7864	0.6877
	1.5	0.2704	0.2079	0.6722	0.4375	0.758	0.6325
	2	0.5638	0.4997	0.8447	0.6925	0.8861	0.8165
25	0.5	0.5696	0.5123	0.8514	0.7155	0.8884	0.8264
	1.5	0.4446	0.4054	0.7936	0.6819	0.8434	0.7918
	2	0.5332	0.4799	0.8474	0.7124	0.8773	0.8165

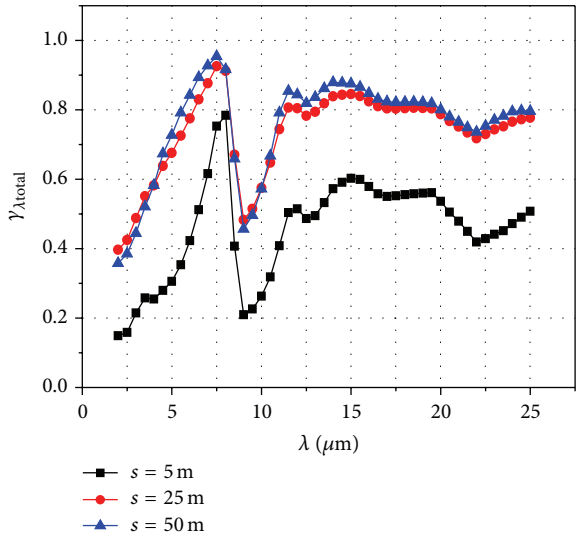

Figure 13: Transmittance variation of total dust under different wavelengths.

large particles caused the spectral transmittance of respirable dust to be higher than that of total dust because large particles are a big part of total dust. As the distance from the dust source increases, the particles system becomes thin and the spectral transmittance is enhanced gradually. Moreover, the relative increase in small particle makes the transmittance values of respirable dust and total dust basically the same.

From the point of wavelength scale, hydroxyl and carboxyl functional groups exist in bituminous coal particles. The absorption peak occurs within the band spectrums of 2–5 and 8–12 μm. Thus, the infrared transmittance of mine dust reaches the highest point at approximately 7.5 μm and the lowest point at approximately 9 μm. The transmittance of particles in different sampling points has similar variation laws as wavelength increases. However, the flank spectrum of the transmittance near the spectral peak is widened as the distance from the dust source increases. Such phenomenon is the transmittance spectrum peak broadening phenomena. This phenomenon is mainly produced when the mine dust concentration decreases; specifically the reduction of large particles scattering contribution weakens the spectrum attenuation effect. Therefore, when conducting remote optical monitoring in long wall working face, to guarantee the effectiveness of the transmitted signal, optical radiation characteristics based on the actual composition of mine dust must be taken as prior data and reasonable detection wavelength bands must be chosen. In view of the bituminous coal particle analyzed above, we should choose the band spectrum of 5–8 μm or 12–25 μm when conducting the optical detection.

6. Conclusion

In this paper, the CFD method is applied to simulate the law of mine dust migration in fully mechanized working faces with dust sources based on two-phase continuous and discrete model. The concentration distribution and dispersion of mine dust are obtained at different locations. According to the occurrence of coal seam in typical working face, we choose the optical constants of bituminous coal particles as infrared complex refractive index parameters of coal dust, combined with Mie scattering theory. Then, we established the optical radiation characteristics simulation method of mine dust and analyzed and summarized the variation law of attenuation, scattering, and transmission spectrum of respirable and total dust particles system along the roadway within the spectral range of 2–25 μm.

The result shows the following: the infrared radiation characteristics of coal dust in working face are directly linked to the concentration, dispersion, and metamorphic degree of coal dust. (1) As the distance from dust source increased, the attenuation and scattering characteristics of respirable dust and total dust along the tunnel have a slight increase and then decline sharply until 25 m after which it remains almost stable; the infrared attenuation of mine dust in the center of the vertical cross-section is generally greater than that at the roof and floor. (2) The attenuation characteristic of respirable dust under the shortwave spectrum is significantly stronger than that in any other spectrum. The absorption effect of functional groups in bituminous coal caused an absorption/transmittance spectrum peak to appear in the infrared wavelengths of mine dust, and the width of the spectral peak varied along with the concentration and dispersion along the tunnel. The results of this paper can lay a scientific

basis and theoretical guidance to the optical remote real-time monitoring of dust pollution sources in mine atmospheric environments.

Conflict of Interests

The authors declare that there is no conflict of interests regarding the publication of this paper.

Acknowledgments

This research was supported by the National Natural Science Foundation of China (Grant nos. 51106175, 51134020, and 51104154) and China Postdoctoral Science Foundation funded project.

References

[1] Z. Wang and T. Ren, "Investigation of airflow and respirable dust flow behaviour above an underground bin," *Powder Technology*, vol. 250, pp. 103–114, 2013.

[2] R. T. Christian, J. B. Nelson, T. E. Cody, E. Larson, and E. Bingham, "Coal workers' pneumoconiosis: in vitro study of the chemical composition and particle size as causes of the toxic effects of coal," *Environmental Research*, vol. 20, no. 2, pp. 358–365, 1979.

[3] R. A. Pinho, F. Bonatto, M. Andrades et al., "Lung oxidative response after acute coal dust exposure," *Environmental Research*, vol. 96, no. 3, pp. 290–297, 2004.

[4] I. Erol, H. Aydin, V. Didari, and S. Ural, "Pneumoconiosis and quartz content of respirable dusts in the coal mines in Zonguldak, Turkey," *International Journal of Coal Geology*, vol. 116-117, pp. 26–35, 2013.

[5] M. Onder and S. Onder, "Evaluation of occupational exposures to respirable dust in underground coal mines," *Industrial Health*, vol. 47, no. 1, pp. 43–49, 2009.

[6] C. K. Man and M. L. Harris, "Participation of large particles in coal dust explosions," *Journal of Loss Prevention in the Process Industries*, vol. 27, no. 1, pp. 49–54, 2014.

[7] M. Mittal, "Limiting oxygen concentration for coal dusts for explosion hazard analysis and safety," *Journal of Loss Prevention in the Process Industries*, vol. 26, no. 6, pp. 1106–1112, 2013.

[8] R. K. Eckhoff, "Does the dust explosion risk increase when moving from μm-particle powders to powders of nm-particles?" *Journal of Loss Prevention in the Process Industries*, vol. 25, no. 3, pp. 448–459, 2012.

[9] Y. Q. Li, Y. P. Qin, X. B. Yang, and L. Tian, "New progress on coal mine dust in recent ten years," *Procedia Engineering*, vol. 26, pp. 738–743, 2011.

[10] http://www.chinasafety.gov.cn/files/2004-12/09/F_42cd456f6-a924f7f8d36815edaa3e531.pdf.

[11] W. Niu and Z. A. Jiang, "Numerical simulation of distribution regularities of dust concentration in fully mechanized top-coal caving face," in *Proceedings of the 4th IEEE International Conference on Bioinformatics and Biomedical Engineering (iCBBE '10)*, pp. 1–4, Chengdu, China, June 2010.

[12] R. Srikanth, *Coal characteristics and respirable dust generation [Ph.D. thesis]*, The Pennsylvania State University, State College, Pa, USA, 1996.

[13] J. C. Kurnia, A. P. Sasmito, and A. S. Mujumdar, "Dust dispersion and management in underground mining faces," *International Journal of Mining Science and Technology*, vol. 24, no. 1, pp. 39–44, 2014.

[14] R. J. Seaney, "Measurement of the mass concentration of airborne dust in coal mines by light-scattering," *Journal of Aerosol Science*, vol. 4, no. 3, pp. 245–251, 1973.

[15] M. Sierakowski, T. R. Woliński, A. W. Domański, and K. Osiñska, "Optical dust sensor for the mining industry," in *Lightmetry 2002: Metrology and Testing Techniques Using Light*, vol. 5064 of *Proceedings of SPIE*, pp. 122–127, Warsaw, Poland, April 2003.

[16] Y. J. Li, *Theoretical and experimental study on particulate density and granularity measurement based on mie scattering theory [Ph.D. dissertation]*, North University of China, Taiyuan, China, 2005, (Chinese).

[17] M. P. Mengüç, S. Manickavasagam, and D. A. D'Sa, "Determination of radiative properties of pulverized coal particles from experiments," *Fuel*, vol. 73, no. 4, pp. 613–625, 1994.

[18] R. Viskanta and M. P. Mengüç, "Radiation heat transfer in combustion systems," *Progress in Energy and Combustion Science*, vol. 13, no. 2, pp. 97–160, 1987.

[19] Y. Yuan, H.-L. Yi, Y. Shuai, F.-Q. Wang, and H.-P. Tan, "Inverse problem for particle size distributions of atmospheric aerosols using stochastic particle swarm optimization," *Journal of Quantitative Spectroscopy and Radiative Transfer*, vol. 111, no. 14, pp. 2106–2114, 2010.

[20] Y. Shuai, S. K. Dong, and H. P. Tan, "Simulation of the infrared radiation characteristics of high-temperature exhaust plume including particles using the backward Monte Carlo method," *Journal of Quantitative Spectroscopy and Radiative Transfer*, vol. 95, no. 2, pp. 231–240, 2005.

[21] F. Wang, Y. Shuai, Y. Yuan, G. Yang, and H. Tan, "Thermal stress analysis of eccentric tube receiver using concentrated solar radiation," *Solar Energy*, vol. 84, no. 10, pp. 1809–1815, 2010.

[22] H.-P. Tan, H.-L. Yi, P.-Y. Wang, L.-M. Ruan, and T. W. Tong, "Ray tracing method for transient coupled heat transfer in an anisotropic scattering layer," *International Journal of Heat and Mass Transfer*, vol. 47, no. 19-20, pp. 4045–4059, 2004.

[23] Z. Zhang, H.-S. Dou, I. Zbicinski, Z. Wu, and J. Liu, "Mathematical modeling of heat and mass transfer in energy science and engineering," *Mathematical Problems in Engineering*, vol. 2013, Article ID 241646, 3 pages, 2013.

[24] H. P. Tan, X. L. Xia, L. H. Liu, and L. M. Ruan, *Numerical Calculation of Infrared Radiation Properties and Transfer*, Harbin Institute of Technology Press, Harbin, China, 2006, (Chinese).

[25] H.-P. Tan and H.-L. Yi, "Temperature response in participating media with anisotropic scattering caused by pulsed lasers," *Journal of Quantitative Spectroscopy and Radiative Transfer*, vol. 87, no. 2, pp. 175–192, 2004.

[26] L. M. Ruan, Q. Z. Yu, L. H. Liu, H. P. Tan, and M. Tang, "A study on coal and ash radiation characteristics parameters," *Journal of Engineering for Thermal Energy and Power*, vol. 18, no. 3, pp. 65–69, 1998 (Chinese).